

## A Diffraction Grating Created in Diamond Substrate by Boron Ion Implantation

A. L. Stepanov<sup>a,b,c\*</sup>, V. I. Nuzhdin<sup>a</sup>, M. F. Galyautdinov<sup>a</sup>,  
N. V. Kurbatova<sup>a</sup>, V. F. Valeev<sup>a</sup>, V. V. Vorobev<sup>b</sup>, and Yu. N. Osin<sup>b</sup>

<sup>a</sup> Kazan E.K. Zavoisky Physicotechnical Institute, Russian Academy of Sciences, Kazan, 420029 Tatarstan, Russia

<sup>b</sup> Kazan Federal University, Kazan, 420008 Tatarstan, Russia

<sup>c</sup> Kazan National Research Technological University, Kazan, 420015 Tatarstan, Russia

\*e-mail: aanstep@gmail.com

Received June 23, 2016

**Abstract**—This work is devoted to new method of manufacturing of diffractive optical elements (gratings). A grating was formed in a diamond substrate by implantation with boron ions through a mask. Ion implantation led to the graphitization of diamond in unmasked regions and resulted in swelling of the irradiated layer. The formation of periodic graphitized surface microstructures on the diamond substrate was confirmed by optical, electron, and atomic force microscopy. The efficiency of operation of the obtained diffractive optical element was demonstrated by probing with He–Ne laser radiation.

DOI: 10.1134/S1063785017010266

The development of modern integral optics requires using new special materials and creating the corresponding technology for manufacturing optical elements and related devices. One topical direction of research is devoted to the development of diamond-based optics [1]. This use of diamond is related to high thermal conductivity and stability under irradiation. Diamond optical elements possess a broad transparency range (0.2- to 5- $\mu\text{m}$  wavelengths) and could operate under conditions of extremal temperature variations and aggressive chemical media. In practice, diamonds are used for manufacturing of diffractive optical elements (DOEs) such as gratings, kinoforms, focusators and correctors, etc. [1, 2]. Diamond DOEs could be used for creating high-power  $\text{CO}_2$  laser-beam converters capable of obtaining radiation power densities up to 20  $\text{kW}/\text{cm}^2$  [3, 4]; photonic-crystal resonators for implementing quantum data storage mechanisms [5]; flux controllers in X-ray optics, e.g., diamond Bragg mirrors with reflection coefficients up to  $\sim 100\%$  [6], etc.

Periodic DOEs on a diamond surface could be created using various technological means, such as exposure to high-power excimer laser pulses [7], etching in transport gas flows [8], etc. In the present work, a new approach has been developed that consists in the formation of periodic diffractive structures on a polished diamond surface by ion implantation through a mask. Previously, this technology has been successfully employed for obtaining DOEs on dielectric and polymer substrates by their implantation with noble metal

ions [9–11]. This particular work was aimed at studying the possibility for formation of DOEs in diamond by implantation with boron ions through a surface mask.

To obtain DOEs on a polished surface of synthetic diamond, the samples were implanted by boron ions with energy of  $E = 40$  keV to a total dose of  $D = 1.43 \times 10^{18}$  ion/ $\text{cm}^2$  at a current density of  $J = 15$   $\mu\text{A}/\text{cm}^2$  on an ILU-3 ion accelerator. Ion implantation was performed through a surface mask representing a nickel grid with a 40- $\mu\text{m}$ -square mesh size. The local morphology and structure of ion-implanted diamond surface were studied by methods of (i) scanning electron microscopy (SEM) on a Merlin instrument (Carl Zeiss) equipped with an HKL NordLys electron backscatter diffraction (EBSD) detector (Oxford Instruments) and (ii) atomic force microscopy (AFM) on a FastScan instrument (Bruker). The optical characteristics of the obtained DOEs were analyzed in a Polar-1 microscope (Mikromed) and by Raman spectroscopy as described previously [12]. The patterns of optical diffraction on DOEs were studied by probing with He–Ne laser radiation at a wavelength of 632.8 nm. The concentration depth profiles for 40-keV boron ion implantation in diamond, which were simulated using an SRIM-2013 algorithm, showed that boron atoms were accumulated in an  $\sim 100$ -nm-thick near-surface layer.

Figure 1 shows images of the grating formed at the surface of diamond implanted with boron ions through a square-mesh mask and observed in (a) an

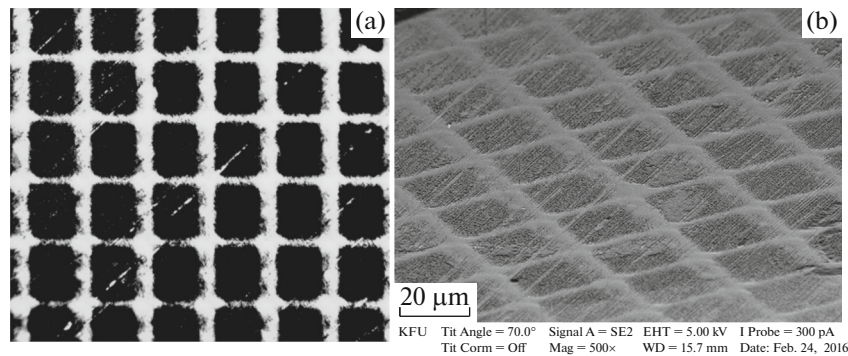


**Fig. 1.** Micrographs of the surface of diamond implanted with boron ions through a square-mesh mask, as observed in (a) an optical microscope and (b) a scanning electron microscope.

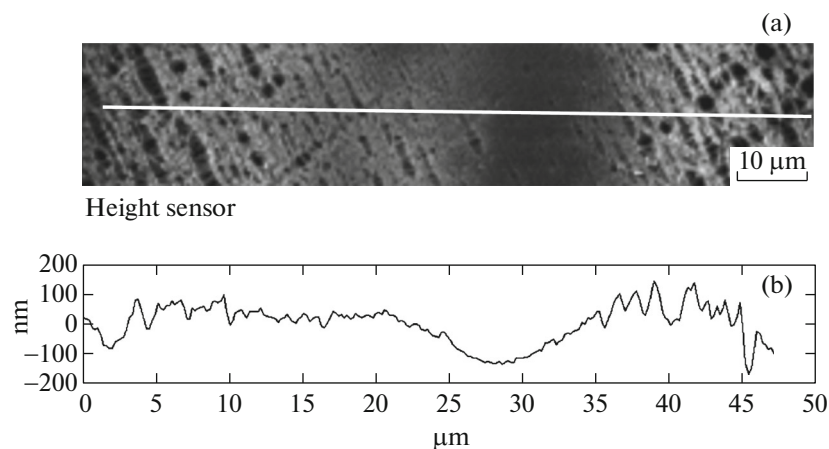


**Fig. 2.** (a) AFM image of a fragment of the diamond grating, showing regions of unimplanted diamond (dark) and boron-implanted cells (bright); white line shows the direction of transverse profile measurement. (b) Surface cross-section profile measured along the line indicated in (a).

optical microscope and (b) a scanning electron microscope at an angle of  $70^\circ$ . As seen, the periodic microstructure comprises dark square cells representing ion-implanted areas separated by spacers (bright regions) of nonimplanted diamond. The size of the implanted regions corresponds to mesh size ( $40\ \mu\text{m}$ ) of the grid mask.

The structural characterization of initial (unimplanted) and boron-implanted regions of diamond was performed by SEM with measurements of EBSD from the near-surface layer of samples. In contrast to the Kikuchi diffraction patterns in the form of lines parallel to planes of the crystalline lattice of diamond, the EBSD patterns from the regions implanted with boron ions exhibit only wide diffuse fringes indicative of the breakage of crystalline lattice and the appearance of amorphous carbon inclusions in the near-surface layer.

Figure 2a shows an AFM image of a fragment of the diamond DOE near the spacer (dark region) between boron-implanted cells (bright rough regions). Figure 2b

presents a surface cross-section profile measured along the line indicated in Fig. 2a. As seen, the boron-implanted regions (cells) protrude by  $\sim 100\ \text{nm}$  above the surface of diamond. This is explained by swelling of the ion-irradiated regions (grating cells) having a lower density ( $\rho_{\text{graphite}} = 2.09\text{--}2.23\ \text{g/cm}^3$ ) as compared to that of nongraphitized diamond ( $\rho_{\text{diamond}} = 3.47\text{--}3.55\ \text{g/cm}^3$ ) [13]. The measurement of Raman spectra excited by an argon laser at a wavelength of  $522\ \text{nm}$  also confirmed the presence of destroyed diamond in boron-implanted material, since the well-known intense line of diamond at  $1336\ \text{cm}^{-1}$  [14] was accompanied by weak lines in the region of  $1560\ \text{cm}^{-1}$  indicative of graphitization [13]. The implantation of boron ions into diamond and destruction of its crystalline lattice may be expected to lead to boron carbide formation as a result of the binding of boron and carbon atoms. However, no characteristic lines corresponding to boron carbide were observed in Raman spectrum in the region from 200 to

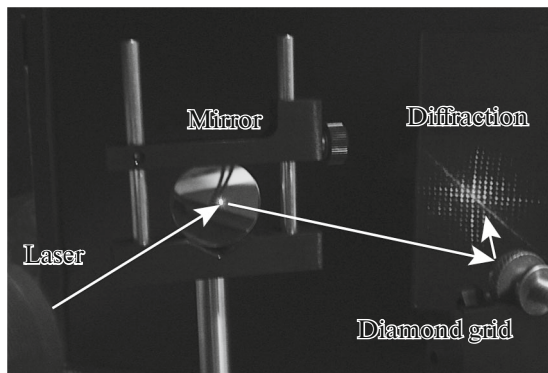


**Fig. 3.** Pattern of reflection diffraction on a boron-implanted diamond grating probed by He–Ne laser radiation. The sample with the grating is mounted on a metal holder.

$1200\text{ cm}^{-1}$  [15]. Nevertheless, according to [16], separate chemical bonds and/or small clusters of boron and carbon atoms (not detected directly by Raman spectroscopy) could be presented in graphitized regions of boron-implanted diamond.

Thus, the implantation of diamond with boron ions leads to both a change in the chemical composition (due to boron accumulation in a sample) and modification of the carbon phase structure (formation of periodic regions of graphitized carbon). Thus, the implantation of boron into diamond through a mask results in the formation of a microstructure with variable distribution of optical constants between diamond spacers (with refractive index  $n_{\text{diamond}} = 2.42$ ) and graphitized cells ( $n_{\text{graphite}} = 2.1\text{--}2.23$ ). Therefore, the obtained periodic microstructure with graphitized regions in diamond substrate could be used as a two-dimensional photonic crystal (DOE). This is illustrated in Fig. 3 by the diffraction image of such a diamond grating probed with He–Ne laser radiation at 632.8-nm wavelength in the reflection geometry. Apparently, by varying the regime of ion implantation and, hence, changing the effective refractive index of modified regions of DOE, it is possible to control optical and diffraction characteristics.

In concluding, we have studied the low-energy high-dose implantation of boron ions into diamond through a surface mask and demonstrated a new method of DOE formation in diamond by this process. As a result, a diffractive microstructure is

obtained at the surface of diamond, in which the phase contrast is formed by regions of graphitized diamond. The main practical application of obtained results is related to the creation and development of new effective elements of diamond optics.

**Acknowledgments.** This work was supported in part by the Russian Foundation for Basic Research, project no. 15-48-02525.

## REFERENCES

1. L. Ratkin, *Fotonika*, No. 4, 18 (2011).
2. V. A. Soifer, *Methods for Computer Design of Diffractive Optical Elements* (Fizmatlit, Moscow, 2003; Wiley, New York, 2002).
3. V. V. Kononenko, V. I. Konov, S. M. Pimenov, A. M. Prokhorov, V. S. Pavel'ev, and V. A. Soifer, *Quantum Electron.* **29**, 9 (1999).
4. M. Karlsson and F. Nikolajeff, *Opt. Express* **11**, 502 (2003).
5. K. N. Tukmakov, B. O. Volodin, V. S. Pavel'ev, et al., *Vestn. Samar. Aerokosm. Univ.* **7** (38), 112 (2012).
6. Y. Shvydko, S. Stopin, V. Blank, and S. Terentev, *Nat. Photon.* **5**, 539 (2011).
7. Yu. K. Verevkin, N. G. Bronnikova, V. V. Korolikhin, Yu. Yu. Gushchina, V. N. Petryakov, D. O. Filatov, N. M. Bituryn, A. V. Kruglov, and V. V. Levichev, *Tech. Phys.* **48**, 757 (2003).
8. A. V. Volkov, N. L. Kazanskii, O. Yu. Moiseev, and V. A. Soifer, RF Patent No. 2197006 (2003).
9. A. L. Stepanov, M. F. Galyautdinov, A. B. Evlyukhin, et al., *Appl. Phys. A* **111**, 261 (2013).
10. A. L. Stepanov, V. I. Nuzhdin, V. F. Valeev, M. F. Galyautdinov, and Yu. N. Osin, RF Patent No. 140494 (2014).
11. M. F. Galyautdinov, V. I. Nuzhdin, Ya. V. Fattakhov, B. F. Farrakhov, V. F. Valeev, Yu. N. Osin, and A. L. Stepanov, *Tech. Phys. Lett.* **42**, 182 (2016).
12. N. V. Kurbatova, M. F. Galyautdinov, N. A. Ivanov, S. S. Kolesnikov, V. L. Papernyi, Yu. N. Osin, and A. L. Stepanov, *Phys. Solid State* **55**, 1899 (2013).
13. R. A. Khmel'nitskii, *Cand. Sci. (Math. Phys.) Dissertation* (Moscow, 2008).
14. A. Deslandes, M. C. Guenette, K. Belay, et al., *Nucl. Instrum. Methods Phys. Res. B* **365**, 331 (2015).
15. A. Hushur, M. Manghnani, H. Werheit, et al., *J. Phys.: Condens. Matter* **28**, 045403 (2016).
16. V. Domnich, S. Reynaud, R. A. Haber, and M. Chhowalla, *J. Am. Ceram. Soc.* **94**, 3605 (2011).

*Translated by P. Pozdeev*